

To be published in Journal of the Optical Society of America B:

Title: THz Emission from a Femtosecond Laser Focus in a Two-Color Scheme

Authors: Alexey Balakin, Alexander Borodin, Igor Kotelnikov, and Alexander Shkurinov

Accepted: 22 October 2009

Posted: 28 October 2009

Doc. ID: 116676



THz Emission from a Femtosecond Laser Focus in a Two-Color Scheme

Alexey V. Balakin¹, Alexander V. Borodin¹, Igor A. Kotelnikov²,

and Alexander P. Shkurinov¹

¹Department of Physics and International Laser Center,

*M.V. Lomonosov Moscow State University,
Leninskie Gory, 119992, GSP-1, Moscow, Russia*

*²Budker Institute of Nuclear Physics,
Lavrentyev Av 11, Novosibirsk, 630090, Russia*

In this paper we critically revise the theory of the four-wave mixing rectification process underlying THz emission from a plasma filament induced by an interaction of two focused femtosecond two-color laser pulses in a gas media. We distinguish a radiation pressure force from a ponderomotive force, discuss conditions for one of these forces to be the dominating contribution to the THz emission and also show that angular distribution of the emitted power critically depends on which of the two forces dominates in a particular experiment. We show that the experimentally observed periodic dependence of the emitted THz power on the gas pressure reveals the dominating role of the radiation pressure force over the ponderomotive force, whereas the angular diagram of the emission allows us to determine the predominant direction of the force. We also emphasize that the THz emission originated by a transient photocurrent exhibits a different dependency from the phase difference between the first and the second harmonics of the optic laser field, which generally enables experimental detection of the prevailing mechanism of the THz emission from the plasma filament. © 2009 Optical Society of America

OCIS codes: 260.3090, 190.2620, 350.5400, 300.2570

1. Introduction

A particular subject of plasma science is to explain various kinds of electromagnetic radiation ranging from THz to x-ray frequencies induced by high-power laser pulses interacting with photoinduced plasma [1, 2]. It has been observed that a broadband electromagnetic pulse (EMP) of THz radiation can be emitted from a plasma filament produced by an ultrashort (less than 100 fsec), high-intensity ($10^{12} \div 10^{15}$ W/cm²) laser pulse propagating in a gas medium [3–5]. Earlier published theories suggest that the basic mechanism behind the THz radiation relies on the effect of a ponderomotive force (PF) which separates electrons from ions spatially within the plasma filament [5, 6] and, consequently, generates a nonlinear electric current. Recently, it has been noted that emitted THz power increases manifold if a two-color scheme is used where a fundamental optical wave with the frequency ω is mixed with its second harmonics (SH) satellite at the doubled frequency 2ω [7–9].

The nonlinear electric current gives rise to the plasma filament polarization. Phenomenological models, formulated in terms of nonlinear polarization susceptibilities, attribute the THz emission to a four-wave mixing (FWM) rectification process [7–12]. The phenomenology describes polarization properties of the THz field reasonably well [9, 13] and the fact that the THz field is subject to the phase difference φ between the fundamental and the SH waves. Specifically, it predicts that $E_{THz} \propto E_{\omega}^2 E_{2\omega} \cos \varphi$ [7, 11, 14, 15] or $E_{THz} \propto E_{\omega}^2 E_{2\omega} \sin \varphi$ [9]. Within the phenomeno-

logical approach it is hardly possible to distinguish whether the $\cos \varphi$ or the $\sin \varphi$ dependency is correct but the latter has been confirmed by experimental studies [9,16]. Furthermore, it has been shown that $E_{THz} \propto E_{2\omega}$ and $E_{THz} \propto E_{\omega}^2$ for sufficiently low fundamental wave energy (less than $100\mu J$) [8,13].

The understanding of plasma formation through optical breakdown has a paramount value for the unveiling of the physical mechanism of the THz emission from an optically generated plasma filament. Earlier dynamic theories of the emission assumed that the photoelectrons, pulled away from gas atoms by strong laser fields, are born with zero macroscopic (i. e. average) velocities [5]. This natural contemplation was disputed in [16,17]. It was suggested that the THz emission at a microscopic level originates from a transient photocurrent created by the photoelectrons produced in a symmetry-broken laser fields composed of a fundamental and a phase-shifted SH optic waves.

In this paper we present a simple theory based on classical assumptions of the THz emission, which takes into account the FWM process. It has led us to the conclusion that the manifold increase of the radiated power, observed in a number of experiments, occurs mainly due to transient photocurrent effect and also due to enhanced plasma production in the process of photoionization, since the multiphoton ionization at doubled frequency goes on faster than at the fundamental frequency. Additional enhancement occurs due to the effect of the plasma pressure force [18]. For the first time, we compute the radiation pressure force (RPF) for a laser pulse

that contains both the first and the second harmonics. We then argue that this newly computed force can produce a larger THz emission even if it is smaller than the PF. At a phenomenological level we also add to the theory the effect of the photocurrent by allowing a non-zero initial macroscopic velocity of the photoelectrons. Though we are not ready at the moment to compute the initial velocity from a strict quantum theory, we present a simple classical consideration of the photoionization process in a two-color laser field, which might hopefully elucidate major properties of the THz emission originated from the photocurrent. In particular, we note that the THz emission, induced by the photocurrent scales as $\sin \varphi$ while that induced by RPF or PF varies in proportion to $\cos \varphi$.

In our model the electrons and ions are initially created by multiphoton ionization (MPI) within laser string, and a dipole moment is subsequently induced in the plasma filament via RPF acting on the electrons and resulting from the velocity-dependent Lorentz force and from PF resulting from spacial inhomogeneity of the laser fields. These forces separate the electrons from the heavy ions both longitudinally and transversely regarding the plasma filament axis on the short time scale of the laser pulse. Behind the laser pulse head the electron fluid oscillates at plasma frequency and generates an EMP propagating away from the plasma filament as first described in [18]. Since plasma frequency is proportional to the square root of the local electron density, and the density varies from point to point within the plasma filament, the frequency spectrum of the THz emission ranges from a maximal value down to almost zero.

The paper is organized as follows. In Section 2 we compute the RPF and then in Section 3 PF. Slow motion of the plasma electrons under the action of these forces that spatially separates the electrons from the ions is analyzed in Section 4 and the resulting THz emission is computed in Section 5. Section 6 adds to our consideration of the effect of the transient photocurrent. The next section 7 specifies experimental apparatus used to validate the theory and our conclusions are summarized in Section 8.

2. Radiation pressure force

To calculate RPF we extend a model first elaborated in [18], where the force was computed for a single-color laser field. In contrast to PF to be analyzed in Section 3, RPF does not explicitly depend on the gradient sizes of the laser beam and, therefore, it dominates for a relatively wide beam. In a single-color scheme, RPF is directed along the laser pulse path [18], whereas a transverse component of the force emerges when a laser pulse at the fundamental frequency ω is mixed with that at the doubled frequency 2ω .

Following [3, 4, 18, 19], we employ an electron-fluid model of the plasma in the presence of the electric and magnetic fields \mathbf{E} and \mathbf{B} , which is governed by the equation

$$m \frac{\partial \mathbf{v}}{\partial t} + m(\mathbf{v} \cdot \nabla) \mathbf{v} = e \mathbf{E} + \frac{e}{c} \mathbf{v} \times \mathbf{B} - \gamma m \mathbf{v} \quad (1)$$

for the fluid velocity \mathbf{v} of the electrons, where e and m are the charge and the mass of the electron, and $-\gamma m \mathbf{v}$ approximates a friction force due to electron scattering by

heavy constituent particles (counting both ions and neutral atoms); throughout the paper, the heavy particles are assumed to remain unmovable.

The RPF indicated below as \mathbf{G} formally originates from a velocity-dependant part of the Lorentz force, i. e. from the second term on the right-hand-side of Equation (1). Since an oscillatory velocity of an electron in the field of a laser pulse is of the order of $v_\omega \sim eE_\omega/m\omega$, and $B_\omega \sim E_\omega$, one formally finds that $G \sim mv_\omega^2/\lambda$, where $\lambda = c/\omega$ is the reduced laser radiation wavelength.

The PF indicated below as \mathbf{F} formally originates from the second term on the left-hand-side of Equation (1), which is evaluated as mv_ω^2/a , with a being a gradient length of the laser pulse envelope. Since $a \gg \lambda$, one might deduce that $G \gg F$ in any circumstances but this would be a rush conclusion because the main term mv_ω^2/λ in G turns out to be zero due to phase cancelation. One can suggest though that the next term in an expansion of G over v_ω can be as large as F or collisional friction can prevent complete phase cancelation.

At the first stage we ignore spatial derivatives in Equation (1) and drop the term $m(\mathbf{v} \cdot \nabla)\mathbf{v}$; it will be retained over again in Section 3. Furthermore, spatial dimensions of the laser string is assumed in this Section to be so enormous that the laser electromagnetic fields $\mathbf{E} = \mathbf{E}_L$ and $\mathbf{B} = \mathbf{B}_L$ can be approximated as spatially uniform over the transverse profile of the plasma filament.

In the rest of this Section we sequentially consider a case of mutually parallel harmonics, $\mathbf{E}_{2\omega} \parallel \mathbf{E}_\omega$, and that of perpendicular harmonics, $\mathbf{E}_{2\omega} \perp \mathbf{E}_\omega$. After having

completed the calculations, we shall see that treatment of these two geometries is sufficient for comprehensive characterization of RPF.

2.A. Case $\mathbf{E}_{2\omega} \parallel \mathbf{E}_\omega$

Let a laser pulse be linearly polarized along the x axis while propagating in air along the positive direction of the z axis, so that

$$\mathbf{E}_L = E_L \hat{\mathbf{x}}; \quad \mathbf{B}_L = E_L \hat{\mathbf{y}}, \quad (2)$$

where $E_L = \frac{1}{2}E_\omega + \frac{1}{2}E_{2\omega} + \text{c.c.}$, and

$$E_\omega = E_1 (t - z/v_g(\omega)) \exp [ik(\omega)z - i\omega t],$$

$$E_{2\omega} = E_2 (t - z/v_g(2\omega)) \exp [ik(2\omega)z - i2\omega t]$$

is the laser beam electric fields at the basic and doubled frequencies, with $t'_1 = t - z/v_g(\omega)$ and $t'_2 = t - z/v_g(2\omega)$ being the retarded times in the reference frames moving with the laser pulse group velocities $v_g(\omega)$ and $v_g(2\omega)$, respectively.

Parameter $1/c$ in Equation (1) formally tracks the order of perturbation theory and reflects the fact that the velocity-dependent Lorentz force is the order of $v/c \ll 1$ smaller than the dominant force due to the electric field under nonrelativistic conditions appropriate here. Then, to zeroth and first orders in the expansion parameter

$1/c$, Equation (1) yields the triplet of equations

$$\begin{aligned} m \frac{\partial v_x}{\partial t} &= e E_L - e \frac{v_z}{c} E_L - \gamma m v_x, \\ m \frac{\partial v_y}{\partial t} &= -\gamma m v_y, \\ m \frac{\partial v_z}{\partial t} &= e \frac{v_x}{c} E_L - \gamma m v_z. \end{aligned} \quad (3)$$

Under the assumption that the electric field envelope E_L varies slowly on the carrier time scale ω^{-1} , the equation for v_x is approximately solved as

$$v_x \approx \frac{e}{2m} \left[\frac{E_\omega}{(\gamma - i\omega)} + \frac{E_\omega^*}{(\gamma + i\omega)} + \frac{E_{2\omega}}{(\gamma - i2\omega)} + \frac{E_{2\omega}^*}{(\gamma + i2\omega)} \right].$$

The equation for v_y means that $v_y = 0$, and the electron motion is limited to the xz plane.

Next, the inspection of the term $e (v_x/c) E_L$ in the equation for v_z reveals that it has the low frequency part

$$G_z = \left\langle e \frac{v_x}{c} E_L \right\rangle = \frac{e^2}{2mc} \frac{\gamma |E_\omega|^2}{(\gamma^2 + \omega^2)} + \frac{e^2}{2mc} \frac{\gamma |E_{2\omega}|^2}{(\gamma^2 + 4\omega^2)} \quad (4)$$

representing RPF along the direction of the laser pulse propagation.

Force (4) has been derived in [18]. It should not be confused with the light pressure force $f_T = \sigma_T (|E_\omega|^2 + |E_{2\omega}|^2) / 8\pi$, where $\sigma_T = (8\pi/3) (e^2/mc^2)^2$ is the Thomson cross section of an electromagnetic wave scattering by a free electron. The light pressure force can be derived from Equation (1) with the radiative reaction force $(2e^2/3c^3) \ddot{\mathbf{v}}$ substituted instead of the friction force $-\gamma m \mathbf{v}$. In most circumstances, the light pressure force is negligibly small, $f_T \ll G_z$.

Straightforward integration of Equation (3) for v_z yields five harmonics, from zeroth to fourth, varying as $e^{\pm i0\omega t}$, $e^{\pm i\omega t}$, $e^{\pm i2\omega t}$, $e^{\pm i3\omega t}$ and $e^{\pm i4\omega t}$, respectively:

$$\begin{aligned}
\frac{v_z}{c} = & \left(\frac{e}{2mc}\right)^2 \left[\frac{E_\omega}{(\gamma - i\omega)} \frac{E_\omega^*}{\gamma} + \frac{E_\omega^*}{(\gamma + i\omega)} \frac{E_\omega}{\gamma} + \frac{E_{2\omega}}{(\gamma - i2\omega)} \frac{E_{2\omega}^*}{\gamma} + \frac{E_{2\omega}^*}{(\gamma + i2\omega)} \frac{E_{2\omega}}{\gamma} \right] \\
+ & \left(\frac{e}{2mc}\right)^2 \left[\frac{E_\omega}{(\gamma - i\omega)} \frac{E_{2\omega}^*}{(\gamma + i\omega)} + \frac{E_\omega^*}{(\gamma + i\omega)} \frac{E_{2\omega}}{(\gamma - i\omega)} + \frac{E_{2\omega}}{(\gamma - i2\omega)} \frac{E_\omega^*}{(\gamma - i\omega)} + \frac{E_{2\omega}^*}{(\gamma + i2\omega)} \frac{E_\omega}{(\gamma + i\omega)} \right] \\
& + \left(\frac{e}{2mc}\right)^2 \left[\frac{E_\omega}{(\gamma - i\omega)} \frac{E_\omega}{(\gamma - i2\omega)} + \frac{E_\omega^*}{(\gamma + i\omega)} \frac{E_\omega^*}{(\gamma + i2\omega)} \right] \\
+ & \left(\frac{e}{2mc}\right)^2 \left[\frac{E_\omega}{(\gamma - i\omega)} \frac{E_{2\omega}}{(\gamma - i3\omega)} + \frac{E_\omega^*}{(\gamma + i\omega)} \frac{E_{2\omega}^*}{(\gamma + i3\omega)} + \frac{E_{2\omega}}{(\gamma - i2\omega)} \frac{E_\omega}{(\gamma - i3\omega)} + \frac{E_{2\omega}^*}{(\gamma + i2\omega)} \frac{E_\omega^*}{(\gamma - i3\omega)} \right] \\
& + \left(\frac{e}{2mc}\right)^2 \left[\frac{E_{2\omega}}{(\gamma - i2\omega)} \frac{E_{2\omega}}{(\gamma - i4\omega)} + \frac{E_{2\omega}^*}{(\gamma + i2\omega)} \frac{E_{2\omega}^*}{(\gamma + i4\omega)} \right].
\end{aligned}$$

The first line here comprises low (zero) frequency terms, the second line contains the first harmonic, i. e. the terms varying as $e^{+i\omega t}$ or $e^{-i\omega t}$, etc. Putting the second and the third lines into the term $e(v_z/c) E_L$ of the equation for v_x gives the low frequency force

$$G_x = \left\langle -e \frac{v_z}{c} E_L \right\rangle = -\frac{e^3}{8m^2c^2} \frac{3\gamma^2}{(\gamma^2 + \omega^2)(\gamma^2 + 4\omega^2)} [E_\omega^2 E_{2\omega}^* + \text{c.c.}], \quad (5)$$

acting in the direction of the laser field polarization.

2.B. Case $\mathbf{E}_{2\omega} \perp \mathbf{E}_\omega$

Let now the SH be polarized perpendicularly to the first harmonic so that

$$\mathbf{E}_L = \frac{1}{2} E_\omega \hat{\mathbf{x}} + \frac{1}{2} E_{2\omega} \hat{\mathbf{y}} + \text{c.c.}, \quad (6)$$

$$\mathbf{B}_L = -\frac{1}{2} E_{2\omega} \hat{\mathbf{x}} + \frac{1}{2} E_\omega \hat{\mathbf{y}} + \text{c.c.}$$

The equations of motion now take the form

$$\begin{aligned}
m \frac{\partial v_x}{\partial t} &= \frac{e}{2} (E_\omega + E_\omega^*) - \frac{e}{2} \frac{v_z}{c} (E_\omega + E_\omega^*) - \gamma m v_x, \\
m \frac{\partial v_y}{\partial t} &= \frac{e}{2} (E_{2\omega} + E_{2\omega}^*) - \frac{e}{2} \frac{v_z}{c} (E_{2\omega} + E_{2\omega}^*) - \gamma m v_y, \\
m \frac{\partial v_z}{\partial t} &= \frac{e}{2} \frac{v_x}{c} (E_\omega + E_\omega^*) + \frac{e}{2} \frac{v_y}{c} (E_{2\omega} + E_{2\omega}^*) - \gamma m v_z.
\end{aligned} \tag{7}$$

Using the same method as in Section 2.A for solving these equations recovers formula

(4) for the longitudinal force G_z . The transverse force

$$\begin{aligned}
G_y &= \left\langle -\frac{e}{2} \frac{v_z}{c} (E_{2\omega} + E_{2\omega}^*) \right\rangle = -\frac{e^3}{8m^2c^2} \left[\frac{E_\omega^2 E_{2\omega}^*}{(\gamma - i\omega)(\gamma - i2\omega)} + \text{c.c.} \right] \approx \\
&\approx \frac{e^3}{16m^2c^2\omega^2} [E_\omega^2 E_{2\omega}^* + \text{c.c.}] \tag{8}
\end{aligned}$$

turns out to be parallel to $\mathbf{E}_{2\omega}$. As shown in Section 2.A, this is also the case for $\mathbf{E}_{2\omega} \parallel \mathbf{E}_\omega$. However, in a general case the transverse force is not exactly parallel to $\mathbf{E}_{2\omega}$ since $G_x/G_y \neq E_{2\omega,x}/E_{2\omega,y}$. For $E_{2\omega,x} = E_{2\omega,y}$ the ratio $G_x/G_y \approx 3\gamma^2/2\omega^2$ is expected to be small. In other words, the effect of SH is stronger when it is polarized differently from the first harmonic.

The longitudinal force G_z is small as compared to G_y provided that the SH is strong enough, $E_{2\omega,y} \gg 4\gamma mc/e$. To evaluate γ we assume that the electron-atom collisions dominate over the electron-ion collisions, which is the case for sufficiently low ionization of the ambient gas in the plasma filament. Then $\gamma = n_a \sigma_{ea} v_e$, where $\sigma_{ea} \sim 10^{-16} \text{ cm}^{-3}$ is the cross section of the electron scattering by neutral atoms, n_a is the atoms density, and the average velocity v_e of the electrons is of the order of their oscillatory velocity $v_\omega \sim eE_\omega/m\omega$.

With these assumptions used, the condition $E_{2\omega} \gg 4\gamma mc/e$ is equivalent to the inequality $E_{2\omega}/E_\omega \gg 4cn_a\sigma_{ea}/\omega \sim 0.2n_a/n_{\text{atm}}$, where $n_{\text{atm}} \approx 3 \times 10^{19} \text{ cm}^{-3}$ is the air density at normal conditions, and $\omega = 2 \times 10^{15} \text{ s}^{-1}$. The condition can be met in a rarefied gas. Furthermore, if it is not satisfied, the transverse force can still produce a more powerful radiation from the plasma filament as shown in Section 5.

Following [20] and [21], many papers refer the estimation $\gamma \approx 10^{12} \div 10^{13} \text{ s}^{-1}$ to the collision rate in the air at atmospheric pressure. This is consistent with the estimation above for the electron energy in the range from 0.1 to 10 eV.

3. Ponderomotive force

We can now retain the term $m(\mathbf{v} \cdot \nabla)\mathbf{v}$ in Equation (1) neglected earlier. Furthermore, we relax the assumption that laser field is spatially uniform over the transverse profile of the plasma filament and retain spatial derivatives of the laser pulse envelope. Specifically, for a linearly polarized laser pulse with given amplitude of the first harmonic

$$E_\omega = E_1(x, y, t - z/v_g(\omega)) \exp[ik(\omega)z - i\omega t]$$

exact expressions for the laser field have the form

$$\begin{aligned} \mathbf{E}_L &= \frac{1}{2}E_\omega \hat{\mathbf{x}} + \text{c.c.}, \\ \mathbf{B}_L &= \frac{1}{2} \frac{kc}{\omega} E_\omega \hat{\mathbf{y}} - \frac{1}{2} \frac{ic}{\omega} \nabla E_\omega \times \hat{\mathbf{x}} + \text{c.c.} \end{aligned} \tag{9}$$

Similar formulae can be drawn for SH. Approximate formulae (2) and (6) are obtained from (9) by dropping ∇E_ω and substituting kc with ω . The PF is identified as the

sum of all terms with spacial derivatives of the pulse envelope, namely

$$\mathbf{F} = -\frac{1}{4}m(\mathbf{v}_\omega^* \cdot \nabla)\mathbf{v}_\omega + \frac{1}{4}\frac{e}{c}\mathbf{v}_\omega^* \times \left[-\frac{ic}{\omega}\nabla E_\omega \times \hat{\mathbf{x}} \right] + \text{c.c.} \quad (10)$$

Straightforward calculations reveal a well known result [22], which takes especially simple form

$$\mathbf{F} = -\frac{e^2}{4m\omega^2}\nabla|E_\omega|^2, \quad (11)$$

if $\gamma = 0$. In plasma physics formula (11) is sometimes called the Miller force. Standard derivation of the Miller force relies on the Lagrangian coordinates where an observer follows individual fluid particles as they move through space (see e.g. [23–25]). On the contrary, Equation (10) gives the Miller force in the Eulerian coordinates that focus on specific locations in the space through which the fluid flows.

The PF can be neglected if $F_z \ll G_z$ and $F_y \ll G_y$.

The first condition is equivalent to the inequality $v_\omega^2/l \ll ev_\omega E_\omega/mc$, where $l = c\tau_L$ is the coherence length of the laser pulse with the time duration τ_L . Putting here $v_\omega \sim eE_\omega/m\omega$, one immediately concludes that the longitudinal PF F_z is small as compared with G_z if $l \gg c/\gamma$. The latter inequality is feasible even for short laser pulses.

The condition $F_y \ll G_y$ leads to the inequality

$$c(E_{2\omega}^2/8\pi)\pi a^2 \gg (c/2r_e)mc^2, \quad (12)$$

where a is a characteristic radius of the plasma filament, and $r_e = e^2/mc^2$ is the

classical electron radius. In other words, the laser power in SH should exceed 4.4 GW for the PF to be smaller than the RPF.

The GW laser power is currently feasible, which provided initial motivation for introducing into account RPF and looking for prospective physical mechanism that could create a dipole moment in the plasma filament [18]. It is worth noting, however, that the transverse part \mathbf{G}_\perp of RPF can produce larger emission from the plasma filament than that of PF \mathbf{F}_\perp even if the ordering (12) fails. Since \mathbf{G}_\perp has a predominant direction across the entire section of the plasma filament, it produces a dipole polarization and, hence, a dipole radiation. On the contrary, \mathbf{F}_\perp is directed mainly towards the center of the filament. It produces therefore a dipole radiation only due to unavoidable ellipticity of the filament cross section. *Ceteris paribus*, a quadrupole radiation is less powerful and it is therefore usually neglected in comparison with the dipole radiation caused by the longitudinal part of the ponderomotive force F_z [5].

4. Slow motion

The combined force $\mathbf{f} = \mathbf{F} + \mathbf{G}$ causes the plasma electrons to execute relatively slow motion which can be characterized by the electron-ion separation vector $\boldsymbol{\xi}$. The latter is associated with the averaged velocity $\langle \mathbf{v} \rangle = \partial \boldsymbol{\xi} / \partial t$ and obeys the equation

$$\frac{\partial^2 \boldsymbol{\xi}}{\partial t^2} + \gamma \frac{\partial \boldsymbol{\xi}}{\partial t} = \frac{e}{m} \mathbf{E} + \frac{\mathbf{f}}{m}. \quad (13)$$

It can be derived from Equation (1) by a straightforward averaging procedure and subsequent dropping the nonlinear term $(\partial \boldsymbol{\xi} / \partial t, \nabla) \partial \boldsymbol{\xi} / \partial t$, which is justified by the

smallness of ξ in comparison with a characteristic radius a of the plasma filament.

The polarization electric field \mathbf{E} in Equation (13) is related to the electron density perturbation δn_e by the equation

$$\operatorname{div} \mathbf{E} = 4\pi e \delta n_e.$$

In turn, δn_e obeys the linearized continuity equation

$$\frac{\partial \delta n_e}{\partial t} + \operatorname{div} \left(n_e \frac{\partial \boldsymbol{\xi}}{\partial t} \right) = 0, \quad (14)$$

which yields

$$\mathbf{E} = -4\pi e n_e \boldsymbol{\xi}. \quad (15)$$

Putting (15) in Equation (13) gives the final equation

$$\frac{\partial^2 \boldsymbol{\xi}}{\partial t^2} + \gamma \frac{\partial \boldsymbol{\xi}}{\partial t} + \omega_p^2 \boldsymbol{\xi} = \frac{\mathbf{f}}{m} \quad (16)$$

for $\boldsymbol{\xi}$, where $\omega_p = \sqrt{4\pi e^2 n_e / m}$ is the plasma frequency, and n_e is the local density of the electrons; in general, the density $n_e = n_e(\mathbf{r}, t)$ varies from point to point and also in time on a timescale different from the period $2\pi/\omega_p$ of the plasma oscillations.

The driving force $\mathbf{f} = \mathbf{f}(\mathbf{r}, t - z/v_g)$ is assumed below to be a function of the radius-vector $\mathbf{r} = (x, y, z)$ and the time $t' = t - z/v_g$ in a co-moving frame of reference. Within a plasma filament, a small difference between the group velocity of the fundamental harmonic, $v_g(\omega) \approx c(1 - \omega_p^2/2\omega^2)$, and that of the second one,

$v_g(2\omega) \approx c (1 - \omega_p^2/8\omega^2)$, can be neglected. Indeed, the mistiming length in the plasma

$$\Delta z_p = \frac{\tau_L}{1/v_g(2\omega) - 1/v_g(\omega)} \approx \frac{8\omega^2}{3\omega_p^2} c \tau_L \quad (17)$$

for the harmonic envelopes E_1 and E_2 to become separated in space is approximately 10^6 times greater than the laser pulse head length $c \tau_L$ for a typical ordering $\omega \sim 10^3 \omega_p$.

As to the mistiming of the harmonics envelopes in the gas, it must be minimized by a proper experimental setup to a negligible amount, since the effect of the second harmonic can not be observed otherwise. For this reason, we substitute v_g below with the speed of light in every occurrence of the retarded time, $t - z/v_g \approx t - z/c$.

On the contrary, in some circumstances the misphasing of the two harmonics should be taken into account. By misphasing we imply the phase factor $\exp [i2k(\omega)z - ik(2\omega)z]$ that enters the term $E_\omega^2 E_{2\omega}^*$ in \mathbf{G}_\perp . Within the plasma filament,

$$\Delta k_p = 2k(\omega) - k(2\omega) \approx -\frac{3}{4} \frac{\omega_p^2}{c\omega}. \quad (18)$$

In a neutral gas,

$$\Delta k_g = \frac{2\omega}{c} [n_\omega - n_{2\omega}] \quad (19)$$

is substantially smaller being proportional to the gas pressure through the refraction indexes of the gas n_ω and $n_{2\omega}$ at corresponding frequencies. The Equation (18) is obtained from (19) by taking $n_\omega = \sqrt{1 - \omega_p^2/\omega^2}$ and $n_{2\omega} = \sqrt{1 - \omega_p^2/(2\omega)^2}$.

Misphasing in the gas determines a relative phase difference φ between the first and

second harmonics at the “entrance” to the plasma filament, whereas the misphasing in the plasma causes modulation of the driving force \mathbf{f} within the filament. The modulation period

$$\ell_p = 2\pi/|\Delta k_p| = 8\pi c\omega/3\omega_p^2 \quad (20)$$

strongly depends on the density of the electron in the plasma filament. In what follows, the modulation is prescribed to the first argument \mathbf{r} of the force $\mathbf{f}(\mathbf{r}, t - z/c)$. The plasma misphasing length ℓ_p substantially exceeds $c\tau_L$ but can be as short as few centimeters.

Integrating Equation (16) over time with the initial conditions $\boldsymbol{\xi} = 0$ and $\partial\boldsymbol{\xi}/\partial t = 0$ at $t = -\infty$ and constant electron density gives

$$\boldsymbol{\xi} = \frac{1}{m\sqrt{\omega_p^2 - \gamma^2/4}} \int_0^\infty \exp[-\gamma\tau/2] \sin\left[\sqrt{\omega_p^2 - \gamma^2/4}\tau\right] \mathbf{f}(\mathbf{r}, t - z/c - \tau) d\tau. \quad (21)$$

The electron density can be approximated by constant in time behind the ionization front of the laser pulse. We will relax this assumption in Sec. 6.

If force \mathbf{f} varies slowly on the time scale ω_p^{-1} , i. e. $\omega_p\tau_L \gg \pi$, Equation (21) reduces to

$$\boldsymbol{\xi} \approx \mathbf{f}(\mathbf{r}, t - z/c) / m\omega_p^2$$

within the laser pulse head, $|t - z/v_g| \lesssim \tau_L$, where the force \mathbf{f} assumes maximal magnitude. Behind the head, $t - z/v_g \gg \tau_L$, the laser pulse excites a damping wake of standing electron plasma oscillations, and

$$\boldsymbol{\xi} \approx -\text{Im} \left\{ \mathbf{f}_{\omega_p} \exp[-(\gamma/2 + i\omega_p)(t - z/c)] \right\} / 2m\omega_p,$$

where \mathbf{f}_{ω_p} is the time Fourier transform

$$\mathbf{f}_{\Omega}(\mathbf{r}) = \int_{-\infty}^{\infty} \mathbf{f}(\mathbf{r}, \tau) e^{i\Omega\tau} d\tau \quad (22)$$

of the driving force at $\Omega = \omega_p$. The current density $\mathbf{j}(\mathbf{r}, t - z/c) = en_e \partial \boldsymbol{\xi} / \partial t$ is calculated by differentiating Equation (21) over time. Keeping only major terms yields

$$\mathbf{j} \approx \frac{en_e}{m} \int_0^{\infty} e^{-\gamma\tau/2} \cos(\omega_p \tau) \mathbf{f}(\mathbf{r}, t - z/c - \tau) d\tau. \quad (23)$$

5. Electromagnetic emission from the plasma filament

In a dipole approximation, the energy spectral intensity of the low frequency radiation generated by the slow motion of the plasma electrons per unit solid angle can be calculated directly from the well-known expression

$$\frac{d\mathcal{E}}{d\Omega d\omega} = \frac{\Omega^2}{4\pi c^3} |\mathbf{n} \times \mathbf{j}_{\Omega, \mathbf{K}}|^2, \quad (24)$$

where \mathbf{n} and $d\omega$ are respectively a unit vector and an element of the solid angle in the direction of radiation, $\mathbf{K} = \mathbf{n}\Omega/c$ is the wave vector, Ω is the low frequency of the emitted radiation, and

$$\mathbf{j}_{\Omega, \mathbf{K}} = \int dt d^3r e^{i\Omega t - i\mathbf{K}\mathbf{r}} \mathbf{j}(\mathbf{r}, t)$$

is the space-time Fourier transform of the current density (see Equation (66.9) in [26]).

Note that Ω is assumed to be positive in Equation (24), where it is already taken into account that $|\mathbf{j}_{\Omega, \mathbf{K}}| = |\mathbf{j}_{-\Omega, -\mathbf{K}}|$. Putting

$$\mathbf{f}(\mathbf{r}, t - z/c - \tau) = \int \frac{d\Omega}{2\pi} \mathbf{f}_{\Omega}(\mathbf{r}) e^{-i\Omega(t - z/c - \tau)}$$

in Equation (23) and then integrating over τ , we obtain the time Fourier transform of the current density

$$\mathbf{j}_\Omega = \frac{e}{2m} n_e \mathbf{f}_\Omega(\mathbf{r}) e^{i\Omega z/c} \left[\frac{1}{\gamma/2 + i\omega_p - i\Omega} + \frac{1}{\gamma/2 - i\omega_p - i\Omega} \right].$$

When taking the spatial Fourier transform of the current, we assume the radius of the plasma filament a to be smaller than the emitted wavelength $2\pi c/\Omega$, so that

$$n_e \approx N_e \delta(x) \delta(y),$$

where $N_e = \iint n_e dx dy$ is the linear density of the electrons in the filament, and δ stands for a delta-function. In this approximation, only the driving force averaged over the filament cross section,

$$\langle \mathbf{f} \rangle = \iint dx dy n_e \mathbf{f} / N_e, \quad \langle \mathbf{f}_\Omega \rangle = \iint dx dy n_e \mathbf{f}_\Omega / N_e,$$

determines radiated power, and the Fourier transform of the current density

$$\mathbf{j}_{\Omega, \mathbf{K}} = \frac{eN_e}{2m} \int \langle \mathbf{f}_\Omega \rangle e^{i(\Omega/c - K_z)z} dz \left[\frac{1}{\gamma/2 + i\omega_p - i\Omega} + \frac{1}{\gamma/2 - i\omega_p - i\Omega} \right], \quad (25)$$

does not depend on the transverse components K_x, K_y of the wave vector. The longitudinal component of the wave vector K_z is related to the angle θ between \mathbf{K} and the axis z of the plasma filament by the equation $K_z = (\Omega/c) \cos \theta$ so that $\Omega/c - K_z = 2(\Omega/c) \sin^2 \theta/2$.

To proceed further, we approximate the dependency of the force $\mathbf{f}(\mathbf{r}, t')$ on the retarded time $t' = t - z/c$ in the head of the laser pulse by a table-like peak with

the duration τ_L so that $\mathbf{f}(\mathbf{r}, t') = \mathbf{f}(\mathbf{r}) H(t' + \tau_L/2) H(\tau_L/2 - t')$, where H stands for the Heaviside step function. Then,

$$\langle \mathbf{f}_\Omega \rangle = \langle \mathbf{f}(\mathbf{r}) \rangle \tau_L \text{sinc}[\Omega\tau_L/2], \quad (26)$$

where $\text{sinc}(\xi) = \sin(\xi)/\xi$. We also take into account that the plasma filament has a finite length L , and some components of the driving force (namely, \mathbf{G}_\perp) can be modulated due to the effect of the misphasing as discussed above. We simulate both these facts by writing

$$\langle \mathbf{f}(\mathbf{r}) \rangle = \mathbf{f}_0 H(z + L/2) H(L/2 - z) \cos[\varphi + \Delta k_p z], \quad (27)$$

where \mathbf{f}_0 is a constant vector, φ is the phase shift between the two harmonics due to optical path difference in the gas, and $\Delta k_p z$ is the phase modulation within the plasma filament. Both φ and Δk_p should be set to zero for the ponderomotive force \mathbf{F} and the longitudinal part of the radiation pressure force G_z .

Performing the integration in Equation (25) and putting the result in Equation (24) gives a bit cumbersome expression

$$\begin{aligned} \frac{d\mathcal{E}}{d\Omega do} = & \frac{\Omega^2}{4\pi c^3} \left(\frac{eN_e L \tau_L}{2m} \right)^2 \frac{(\gamma^2/4 + \Omega^2) \text{sinc}^2(\Omega\tau_L/2)}{(\gamma^2/4 + (\omega_p - \Omega)^2)(\gamma^2/4 + (\omega_p + \Omega)^2)} \times \\ & \times \left\{ \left[\text{sinc} \left(\frac{\Omega L}{c} \sin^2 \frac{\theta}{2} + \frac{\Delta k_p L}{2} \right) + \text{sinc} \left(\frac{\Omega L}{c} \sin^2 \frac{\theta}{2} - \frac{\Delta k_p L}{2} \right) \right]^2 \cos^2 \varphi + \right. \\ & \left. + \left[\text{sinc} \left(\frac{\Omega L}{c} \sin^2 \frac{\theta}{2} + \frac{\Delta k_p L}{2} \right) - \text{sinc} \left(\frac{\Omega L}{c} \sin^2 \frac{\theta}{2} - \frac{\Delta k_p L}{2} \right) \right]^2 \sin^2 \varphi \right\} |\mathbf{n} \times \mathbf{f}_0|^2. \end{aligned} \quad (28)$$

It simplifies to

$$\frac{d\mathcal{E}}{d\Omega do} = \frac{\Omega^2}{4\pi c^3} \left(\frac{eN_e L \tau_L}{m} \right)^2 \frac{(\gamma^2/4 + \Omega^2) \text{sinc}^2(\Omega\tau_L/2)}{(\gamma^2/4 + (\omega_p - \Omega)^2)(\gamma^2/4 + (\omega_p + \Omega)^2)} \times \\ \times \text{sinc}^2\left(\frac{\Omega L}{c} \sin^2 \frac{\theta}{2}\right) \cos^2 \varphi |\mathbf{n} \times \mathbf{f}_0|^2, \quad (29)$$

if $\Delta k_p L/2 \ll 1$, that is if the plasma filament length is substantially smaller than the modulation length (20), $L \ll \ell_p$.

This constitutes our principal result describing the spectral and angular distribution of the radiation.

The frequency spectrum has a maximum at the plasma frequency, corresponding to $\omega_p/2\pi \sim 1$ THz for $n_e = 10^{16} \text{ cm}^{-3}$. Experimental data exhibit a broadband frequency spectrum rather than resonant-like one. It would mean either that the friction coefficient γ is comparable with ω_p or that the variation ω_p across the plasma filament cross section should be taken into account. This can be done by averaging $\mathbf{f}/[\gamma/2 \pm i\omega_p - i\Omega]$ in Equation (25) rather than just the force \mathbf{f} alone. In our opinion, both these effects are equally important.

Though being wide, the frequency spectrum in most experiments with femtosecond lasers is narrower than one could evaluate from the spectral width π/τ_L of the seed laser pulse. It means that exact shape of the seed pulse is not very important, and the factor $\text{sinc}^2(\Omega\tau_L/2)$ can be dropped from Equations (28) and (29) as it is approximately equal to 1 within the main part of the spectrum. We utilize this observation in the next Section.

As it is seen from Equations (28) and (29), the emitted THz power is affected by the phase difference φ between the fundamental and second-harmonic pulses caused by the dispersion of the refractive index along the path of these optical pulses in the gas to the foci, as reported by Cook and Hochstrasser [7] and later by Kress et al. [9] and Chen et al. [27]. Furthermore, Equation (28) also describes the effect of the dispersion inside the plasma filament, and the latter limits the effective length of the filament that contributes to the THz emission. In particular, Equation (29) predicts that the total emitted power oscillates from zero to a maximal value as the phase shift φ varies with the gas pressure. More accurate Equation (28) excludes falling the emitted power down to zero as the result of phase modulation within the plasma filament. Instead of being zero, total radiated power falls down to a minimal value, which depends on the ratio of the plasma filament length L to the modulation length ℓ_p . Since $\varphi = 0$ both for the ponderomotive force and longitudinal radiation pressure force, detecting the power oscillations would certainly indicate that the transverse radiation pressure force plays dominating role in the emission of the THz waves from the plasma filament. It is remarkable that maximal emitted power is proportional to the square of the total number $N_e L$ of the free electrons in the plasma filament.

The angular distribution also provides crucial information regarding which of the two forces plays dominating role. According to Equation (29), the angular distribution contains multiple lobes, the angular positions of which are defined by the condition $2L \sin^2 \theta/2 = N\lambda$ for the emitted wavelength $\lambda = 2\pi c/\Omega$ and integer number $N =$

0, 1, 2,

The lobe $N = 0$ does not exist if the force \mathbf{f}_0 is directed along plasma filament. This occurs when the longitudinal force is greater than the transverse one, i. e. $f_z \gg f_\perp$. In this case, the angular distribution is proportional to $\sin^2 \theta \operatorname{sinc}^2 (\Omega L \sin^2(\theta/2)/c)$, and the main lobe, $N = 0$, is empty inside resembling inverse Cherenkov cone as shown in Fig. 1(a) for the case $L/\lambda = 50$. The lobe $N = 1$ is the strongest and corresponds to the cone opening angle

$$\theta \approx \sqrt{2\lambda/L} \quad (30)$$

On the contrary, if the transverse force is dominant, i. e. $f_\perp \gg f_z$, the angular distribution is proportional to $(1 - \sin^2 \alpha \sin^2 \theta) \operatorname{sinc}^2 (\Omega L \sin^2(\theta/2)/c)$, where α is the azimuthal angle (around the filament axis z) counted from the direction \mathbf{f}_\perp . In this case, the main lobe is filled. It is also slightly distorted in azimuthal direction but this distortion is very weak since $(1 - \sin^2 \alpha \sin^2 \theta) \approx 1$ for small θ . In addition, the contribution of the longitudinal force is suppressed by the small factor $\sin^2 \theta \sim 2\lambda/L$. It means that domination of the transverse force over the longitudinal one requires a less severe condition $f_\perp \gg f_z \times (\lambda/L)$ to be satisfied instead of the inequality $f_\perp \gg f_z$ specified above from superficial consideration.

Comparing the Figs. 1(a) and 1(b) shows that measuring angular distribution of the radiated power allows determining dominant direction of the driving force \mathbf{f} . However, it is important to note that the contribution of the transverse ponderomotive

force \mathbf{F}_\perp to the emitted power is substantially suppressed and might seem to be lower than that of the radiation pressure force \mathbf{G}_\perp of same magnitude. It follows from the fact that $\iint n_e \nabla_\perp |E_\omega|^2 dx dy = 0$ for an axisymmetric distribution of both n_e and $|E_\omega|^2$.

The angular distribution becomes even more complicated if $\ell_p \sim L$, when exact formula (28) should be used instead of (29). In this case, not only the total emitted power varies with the gas pressure (through the phase shift φ) but also the angular distribution does. A more certain conclusion that follows from Equation (28) is that it predicts drastic decrease of the emitted power when the plasma filament length greatly exceeds the modulation length, $L \gg \ell_p$. In this case, the terms in the curly brackets drop as $(\ell_p/L)^2$, and the total power occurs to be proportional to $(N_e \ell_p)^2$ instead of $(N_e L)^2$. Thus, ℓ_p is an effective length of the plasma filament that effectively contributes to the radiation.

6. The effect of the transient photocurrent

We now relax the assumption that photoelectrons are born with zero average velocity. Though the multiphoton ionization is essentially a quantum process, we employ a simple classical model in a hope that it catches such crucial feature of the photoionization as the dependency on the phase shift φ between the first and second harmonics of the laser field.

Let us consider motion of a free electron in the two-color laser field

$$E(t) = E_\omega \cos(\omega t) + E_{2\omega} \cos(2\omega t + \varphi). \quad (31)$$

We assume that the electron is born in the result of multiphoton ionization at the instant of time t_N and that its velocity at that moment is equal to zero. Then, we have

$$v(t) = v_\omega \sin(\omega t) + \alpha v_\omega \sin(2\omega t + \varphi) + v_N \quad (32)$$

for $t > t_N$, where $v_\omega = eE_\omega/m\omega$, and $\alpha = E_{2\omega}/E_\omega$. The last term in Equation (32), which does not depend on time, is set by the condition $v(t_N) = 0$ and turns out to be the average velocity of the electron in the laser field:

$$v_N = -v_\omega \sin(\omega t_N) - \alpha v_\omega \sin(2\omega t_N + \varphi). \quad (33)$$

Employing the classical model of of the photocurrent generation [16,17], we make one more preposition, validity of which we will discuss later. Namely, we assume that due to extremely large nonlinearity of the multiphoton ionization process tearing-off a bound electron from an atom occurs exclusively at the instants of time, corresponding the maximums of the absolute magnitude of the electric field strength. Making use of the smallness of the parameter $\alpha = E_{2\omega}/E_\omega$ in realistic experimental conditions, we find the phase of the fundamental harmonic at these instants of time,

$$\omega t_N = \pi N - 2\alpha \sin \varphi \cos \pi N, \quad (34)$$

where N stands for an integer. Having calculated average velocity of an electron

$$v_N = \frac{3}{2} \alpha v_\omega \sin \varphi \quad (35)$$

born at these moments, we note that it does not depend on N and, hence, is the same both for odd and even maximums. However, own these maximums have different magnitudes:

$$E_N \equiv |E(t_N)| = |E_\omega| [1 + \alpha \cos \pi N]. \quad (36)$$

Respectively, the number of the electrons produced at odd and even maximums are different.

Generally speaking, this difference might be very huge even for very small ratio α , since a photon with doubled frequency has doubled energy and, thus, a two times smaller number of such photons is required to complete the act of ionization. However, for the sake of simplicity we assume that the parameter α is so small that the photoionization is produced exclusively by the fundamental harmonic of the laser field. It is then reasonable to think that the number of the electrons produced in the odd maximums differs from that produced in the even ones by the value of the order of α . If it is not so and the ionization by the second harmonic dominates over the fundamental harmonic, one needs to think that the electrons are predominantly born at the maximums of the second harmonic but we will not consider this case. Since the number of the electrons produced at different moments differs by a small amount of order of α according to our assumption, the difference can be neglected

when calculating the total (macroscopic) initial momentum of the electrons because their average velocity (35) itself contains the small parameter α . We note also that any initial spread of the electron velocities does not appear in our model. It means that a hydrodynamic approximation with zero temperature can be used to describe further motion of the electron fluid.

To include the effect of the initial electron velocity, we extend the equations of slow motion from Sec. 4. First, we need to add a source producing \dot{n} electrons per unit of time in a unit of volume and take into account that the electrons acquire an initial velocity \mathbf{v}_0 when they are born. Respectively, we add the term \dot{n} to the R.H.S. of the continuity equation:

$$\frac{\partial n_e}{\partial t} + \text{div}(n_e \mathbf{v}) = \dot{n}, \quad (37)$$

and the summand $\dot{n} \mathbf{v}_0$ to the R.H.S. of the equation of motion:

$$\frac{\partial}{\partial t} n_e \mathbf{v} + \nabla \cdot (n_e \mathbf{v} \mathbf{v}) = \frac{en_e}{m} \mathbf{E} - \gamma n_e \mathbf{v} + n_e \frac{\mathbf{f}}{m} + \dot{n} \mathbf{v}_0.$$

Recall that \mathbf{E} stands here for a slow polarization field appeared due to spatial separation of the electrons from neutralizing ion background. Excluding $\partial n_e / \partial t$ from the second equation with the aid of the first one, we obtain

$$\frac{\partial}{\partial t} \mathbf{v} + (\mathbf{v} \cdot \nabla) \mathbf{v} = \frac{e}{m} \mathbf{E} - \gamma \mathbf{v} + \frac{\mathbf{f}}{m} + \frac{\dot{n}}{n_e} [\mathbf{v}_0 - \mathbf{v}]. \quad (38)$$

To proceed further, we linearize Equations (37) and (38), assuming the velocity \mathbf{v} and the perturbation of the electron density δn_e to be equally small quantity. By an

unperturbed electron density we shall imply the quantity

$$n = \int_{-\infty}^t \dot{n}(t) dt, \quad (39)$$

which is formal solution of the continuity equation for $\mathbf{v} \equiv 0$. In a focus of a femtosecond laser pulse, secondary ionization has no time to enter the scene and the source of the electrons \dot{n} can therefore be considered as a given function of time. Taking this fact into account when linearizing Equations (37) and (38), putting there $n_e = n + \delta n_e$ and expressing the velocity $\mathbf{v} = \partial \boldsymbol{\xi} / \partial t$ through the vector $\boldsymbol{\xi}$, we obtain

$$\frac{\partial \delta n_e}{\partial t} + \text{div} \left(n_e \frac{\partial \boldsymbol{\xi}}{\partial t} \right) = 0, \quad (40)$$

$$\frac{\partial^2 \boldsymbol{\xi}}{\partial t^2} + \gamma \frac{\partial \boldsymbol{\xi}}{\partial t} = \frac{e}{m} \mathbf{E} + \frac{\mathbf{f}}{m} + \frac{\dot{n}}{n} \left[\mathbf{v}_0 - \frac{\partial \boldsymbol{\xi}}{\partial t} \right]. \quad (41)$$

Since Equation (40) exactly coincides with Equation (14) from Section 4, the expression (15) for the polarization electric field \mathbf{E} also remains valid. Putting it in Equation (41) gives the final equation

$$\frac{\partial^2 \boldsymbol{\xi}}{\partial t^2} + \gamma \frac{\partial \boldsymbol{\xi}}{\partial t} + \omega_p^2 \boldsymbol{\xi} = \frac{\mathbf{f}}{m} + \frac{\dot{n}}{n} \left[\mathbf{v}_0 - \frac{\partial \boldsymbol{\xi}}{\partial t} \right] \quad (42)$$

for $\boldsymbol{\xi}$, where $\omega_p = \sqrt{4\pi e^2 n / m}$ is again the plasma frequency. This equation differs from Equation (16) by the last term in R.H.S. The driving force $\mathbf{f} = \mathbf{f}(\mathbf{r}, t - z/v_g)$ again can be interpreted as a function of the radius-vector $\mathbf{r} = (x, y, z)$ and the time $t' = t - z/v_g$ in a co-moving frame of reference. The same assumption is also applicable to the quantities n and \mathbf{v}_0 .

Integrating Equation (42) over time should be done with the initial conditions $\boldsymbol{\xi} = 0$ and $\partial\boldsymbol{\xi}/\partial t = 0$ at $t = -\infty$. Since both the plasma density n , the plasma frequency ω_p , the driving force \mathbf{f} and the initial velocity \mathbf{v}_0 depend on time, the integration can be generally done only numerically. There is, however, a practically important case, when one can present an approximate solution.

As it has been noted in the end of Section 4, the period $2\pi/\omega_p$ of the plasma oscillations in present-day experiments with femtosecond lasers does not exceed the duration of the laser pulse. Restricting ourselves to the solution of Equation (42) at larger times, we can say that the separation vector $\boldsymbol{\xi}$ in an arbitrary point with the coordinate z starts to differ from zero only after laser pulse head passing through the point, i.e. at $t > z/v_g$. Behind the pulse head the unperturbed electron density remains constant as well as the plasma frequency. As the result, Equation (42) is transformed into the ordinary differential equation

$$\frac{\partial^2 \boldsymbol{\xi}}{\partial t^2} + \gamma \frac{\partial \boldsymbol{\xi}}{\partial t} + \omega_p^2 \boldsymbol{\xi} = 0 \quad (43)$$

with zero right-hand-side and constant coefficients, which depend of the point coordinates only as on parameters. This equation should be solved with the initial conditions

$$\boldsymbol{\xi} = 0, \quad (44)$$

$$\frac{\partial \boldsymbol{\xi}}{\partial t} = \frac{1}{n} \int [n \mathbf{f}/m + \dot{n} \mathbf{v}_0] dt \quad (45)$$

at $t = z/v_g + 0$. It is assumed here that n before the integral sign in the R.H.S. of (45)

is the electron density established after the laser pulse head passing, and the range of the integrations over the time comprises the entire interval of the pulse passing (e.g., from $t = z/v_g - \tau_L$ to $t = z/v_g + \tau_L$). The solution of the reduced problem (43)–(45) is trivial:

$$\xi = \frac{e^{-\gamma(t-z/v_g)/2}}{\sqrt{\omega_p^2 - \gamma^2/4}} \sin \left[\sqrt{\omega_p^2 - \frac{\gamma^2}{4}} \left(t - \frac{z}{v_g} \right) \right] \frac{\partial \xi}{\partial t} \Big|_{t=z/v_g+0}. \quad (46)$$

Elementary comparison of the summands in the integrand in Equation (45) shows that the effect of initial electron momentum acquired by the electrons at the act of the ionization causes stronger plasma polarization if the momentum exceeds the momentum gained by the electrons from the driving force for the entire duration of the laser pulse, i.e. $mv_0 \gg f\tau_L$. A formal estimation $v_0 \sim \alpha v_\omega$, following from the classical treatment in the beginning of this Section, leads to the conclusion that the condition $mv_0 \gg f\tau_L$ is satisfied practically for any laser power feasible to the date. However, available quantum theories predict a substantially lower value of v_0 , especially in the case of the laser pulse with the duration significantly exceeding the period of the laser field, $\omega\tau_L \gg 1$.

Indeed, the notion of the instant of time of the ionization has no evident sense in quantum physics. According to the uncertainty principle, the instant of time of the ionization is determined at most with the accuracy of the order of the period of the bound electron gyration around the atomic core $2\pi/\omega_a$ (if the frequency $\omega_a = J/\hbar$, corresponding to the ionization potential J can be interpreted so) or

with the accuracy of the ionizing field period $2\pi/\omega$. As a quantum theory of the photoionization [28, 29] says, the ionization occurs at times close to the absolute maximum of the laser field (with account of the field envelope time profile) in a so called limit of low frequency, when $v_\omega \gg v_e = \sqrt{2J/m}$. [30] According to the results of Ref. 29, the velocity distribution of the produced electrons has a maximum near $v_{\max} = \int_0^\infty dt eE(t)/m$. Though the computation in Ref. 29 was performed for a special case, where $E(-t) = E(t)$, which corresponds to the phase shift φ , multiple of π , its result assumes that v_{\max} drops quickly as the pulse duration increases, since the integral $\int_0^\infty dt eE(t)/m$ decreases in proportion to $1/\omega\tau_L$ for a pulse with table-like time envelope and even more quickly for smoother envelope profiles. For example, it gives $v_{\max} \propto \exp(-1/\omega^2\tau_L^2)$ for the Gauss profile. For a monochromatic wave, the theory yields $v_{\max} = 0$.

On the other hand, a numerical solution of the Schrödinger and experimental data, reported in Ref. 31, support the dependency of the average velocity on the phase shift proportional to $\sin \varphi$, as predicted by our simple classical model. However, the same result contradicts to the results of Ref. 29 as the latter gives nonzero v_{\max} for $\varphi = \pi N$.

7. Experimental results and discussion

An experimental evidence is needed to establish veracity of the model presented above.

We used experimental scheme analogous to that described in Reference [7].

We employed an amplified Ti:sapphire laser system providing fundamental 120 fs and 800 nm pulses at the repetition rate of 1 kHz. The second harmonic is generated in a beta barium borate crystal (BBO, type-I, 300 μm thick). Both the intense fundamental laser pulses and their second-harmonic descendants are focused into a gas cell by a lens with focal length of $f = 18$ cm. Radiated terahertz waves are collected by a set of crystal quartz lenses and then focused by an off-axis parabola ($f = 25$ mm) onto 300 μm -thick $\langle 110 \rangle$ oriented ZnTe crystal for electro-optical detection. The metal gas cell of 100 mm length has a window with diameter of 25 mm. The front window is made of a 300 μm thick fuses quartz plate and a rear window is fabricated from teflon. The gas cell is filled with air or with a noble gas (either argon, neon, xenon or krypton) at adjustable pressure in the range from 0 to 1.5 bar. Pure gas can be pumped into or evacuated from the cell through a gas diluting system. To separate and reduce contribution of the THz wave from the BBO crystal, we used an adjustable special filter placed inside the gas cell in the focus area.

According to basic principles of the THz time domain measurements, the temporal profile of the emitted THz wave is measured by scanning the time delay of a probe beam at the fundamental frequency ω relative to the THz pulse. The phase shift φ between the fundamental and the SH pulses can be changed [7, 9, 11] by varying the distance Δl between SHG (BBO) crystal and the laser focus. In addition, φ varies with the gas pressure in the cell since both $n_\omega - 1$ and $n_{2\omega} - 1$ are proportional to the pressure but with different coefficients of proportionality. In both cases, modulation

of the THz wave amplitude has been detected in accordance with Equation (28). Similar behavior has been also observed by Kress et al [9] who moved a SH nonlinear crystal (BBO) away or to the focus. In this case the phase shift can be written as $\varphi = (2\omega/c) (n_\omega - n_\omega) \Delta l$.

The variation of the phase shift leads also to the changes of the temporal profile of the THz field and their polarity [11, 16] in agreement with our discussion in the end of Section 5. In our experiments, the phase shift changes by π as the gas (Xe) pressure changes by an amount in the range from 0.6 to 0.7 bar.

Figure 2 illustrates this statement.

Using indexes of refraction from [32–35], we have estimated the pressure periods to be 1.1, 0.6, 0.25 and 10 atm for Ar, Kr, Xe and Ne, respectively. These estimates fairly agrees with experimentally observed values, especially at lower pressures.

8. Conclusion

In the paper we discussed basic principles of the terahertz waves generation initiated by the optical breakdown in air of a noble gas. We focussed mainly on the two-color scheme of the THz wave generation. We presented a simple classical model of the multiple photoionization in a two-color laser field that hopefully catches some peculiar features of the process. In particular, we emphasize that the contribution of the radiation pressure force to the emitted THz power varies with the phase shift φ due to optical phase difference in the air to the laser focus in proportion to $\cos \varphi$,

whereas the contribution of the transient photocurrent is proportional to $\sin \varphi$.

We have distinguished the radiation pressure force from the ponderomotive force and, for the first time, have calculated the transverse component of the radiation pressure force.

We have shown that the effect of the second harmonic is stronger when it is polarized differently from the first harmonic. In addition, the effect of the transverse ponderomotive force is suppressed as compared with the effect of the transverse radiation pressure force because the ponderomotive force varies across the section of the laser beam. Furthermore, the effect of the longitudinal driving force is suppressed as compared to transverse force by the factor λ/L .

Both empty and filled angular diagram of the THz emission (see Fig. 1) are allowed by our theory and both types of the diagram were observed experimentally though no special care has been taken so far to quantitatively validate experimental data against our theory (as it was not available earlier). By inspecting the angular diagram of the THz radiation, one can deduce which component, the longitudinal or the transverse, makes dominating contribution to the emitted THz power.

We showed that the effective length ℓ_p (given by Equation (20)) of the emitting part of the plasma filament is related to angle spread of the THz radiation angular diagram if $\ell_p \ll L$. We explained that the effective length shortens due to optical dispersion within the filament in inverse proportion to the electron density.

We attributed the broadband character of the THz radiation to special inhom-

geneity of the electron density within the plasma filament.

If we compare our theoretical speculations with complete experimental data available so far, we conclude that they do not allow validating our theory without doubts since some experimental results are mutually exclusive. We hope that future experiments will resolve this discrepancy.

The authors are grateful to Dr. V. Davydenko for consulting us regarding properties of the laser-induced plasma, Prof. X.-C. Zhang and Prof. A.B. Savelev for useful discussions of various aspects of the laser-induced THz radiation and Dr. M. Nazarov for the assistance in the experiments.

This work was supported by the Russian Foundation for Basic Research in the frameworks of the grants No RFBR 08-02-00869, 09-02-12198 and by the Russian Federal Agency for Science and Innovation (Rosnauka), the state contract 02.740.11.0223.

References

1. P. Sprangle, E. Esarey, and A. Ting, “Nonlinear theory of intense laser-plasma interactions,” *Phys. Rev. Lett.* **64**, 2011–2014 (1990).
2. P. B. Corkum, “Plasma perspective on strong field multiphoton ionization,” *Phys. Rev. Lett.* **71**, 1994–1997 (1993).
3. H. Hamster, A. Sullivan, S. Gordon, W. White, and R. W. Falcone, “Subpicosecond, electromagnetic pulses from intense laser-plasma interaction,” *Phys. Rev. Lett.* **71**, 2725–2728 (1993).
4. H. Hamster, A. Sullivan, S. Gordon, and R. W. Falcone, “Short-pulse terahertz radiation from high-intensity-laser-produced plasmas,” *Phys. Rev. E* **49**, 671–677 (1994).
5. P. Sprangle, J. R. Peñano, B. Hafizi, and C. A. Kapetanacos, “Ultrashort laser pulses and electromagnetic pulse generation in air and on dielectric surfaces,” *Phys. Rev. E* **69**, 066415 (2004).
6. L. M. Gorbunov and A. A. Frolov, “Emission of low-frequency electromagnetic waves by a short laser pulse in stratified rarefied plasma,” *Journal of Experimental and Theoretical Physics* **83**, 967–973 (1996).
7. D. J. Cook and R. M. Hochstrasser, “Intense terahertz pulses by four-wave rectification in air,” *Optics Letters* **25**, 1210–1212 (2000).
8. T. Bartel, P. Gaal, K. Reimann, M. Woerner, and T. Elsaesser, “Generation of

- single-cycle THz transients with high electric-field amplitudes,” *Optics Letters* **30**, 2805–2807 (2005).
9. M. Kress, T. Loeffler, M. D. Thomson, R. Doerner, H. Gimpel, K. Zrost, T. Ergler, R. Moshhammer, U. Morgner, J. Ullrich, and H. G. Roskos, “Determination of the carrier-envelope phase of few-cycle laser pulses with terahertz-emission spectroscopy,” *Optics Letters* **29**, 1120–1122 (2004).
10. N. Bloembergen, “Recent progress in four-wave mixing spectroscopy,” in “Laser Spectroscopy,” , vol. IV of *Laser Spectroscopy*, H. Walther and K. W. Rothe, eds. (Springer, Berlin, 1979), vol. IV of *Laser Spectroscopy*, pp. 340–348.
11. X. Xie, J. Dai, and X.-C. Zhang, “Coherent control of thz wave generation in ambient air,” *Physical Review Letters* **96**, 075005 (2006).
12. J. Reintjes, *Nonlinear Optical Parametric Processes in Liquids and Gases* (Academic, New York, 1984), second edition ed.
13. A. Houard, Y. Liu, B. Prade, and A. Mysyrowicz, “Polarization analysis of terahertz radiation generated by four-wave mixing in air,” *Opt. Lett.* **33**, 1195–1197 (2008).
14. J. Dai, X. Xie, and X.-C. Zhang, “Detection of broadband terahertz waves with a laser-induced plasma in gases,” *Physical Review Letters* **97**, 103903 (2006).
15. X. Lu, N. Karpowicz, and X.-C. Zhang, “Broadband terahertz detection with selected gases,” *J. Opt. Soc. Am. B* **26**, A66–A73 (2009).

16. K. Y. Kim, J. H. Glowina, A. J. Taylor, and G. Rodriguez, “Terahertz emission from ultrafast ionizing air in symmetry-broken laser fields,” *Opt. Express* **15**, 4577 (2007).
17. M. Kress, T. Loëffler, M. D. Thomson, R. Doérner, H. Gimpel, K. Zrost, T. Ergler, R. Moshhammer, U. Morgner, J. Ullrich, and H. G. Roskos, “Determination of the carrier-envelope phase of few-cycle laser pulses with terahertz-emission spectroscopy,” *Nature Physics* **2**, 327–331 (2006).
18. C.-C. Cheng, E. M. Wright, and J. V. Moloney, “Generation of electromagnetic pulses from plasma channels induced by femtosecond light strings,” *PRL* **87**, 213001 (2001).
19. N. Bloembergen, R. K. Chang, S. S. Jha, and C. H. Lee, “Optical second-harmonic generation in reflection from media with inversion symmetry,” *Phys. Rev.* **174**, 813–822 (1968).
20. A. Proulx, A. Talebpour, S. Petit, and S. L. Chin, “Fast pulsed electric field created from the self-generated filament of a femtosecond ti:sapphire laser pulse in air,” *Optics Communications* **174**, 305–309 (2000).
21. J. F. Ready, *Effects of High Power Laser Radiation* (Academic Press, New York, 1971).
22. G. A. Askar’yan, “Cherenkov radiation from optical pulses,” *Phys. Rev. Lett.* **57**, 2470 (1986).

23. B. B. Kadomtsev, *Collective Phenomena in Plasmas* (Pergamon Press, New York, 1982).
24. L. A. Artsimovich and R. Z. Sagdeev, *Plasma physics for physicists* (Atomizdat, Moscow, 1979). In Russian.
25. R. Fitzpatrick, *The Physics of Plasmas* (Lulu, 2008).
26. L. D. Landau and E. M. Lifshitz, *The classical theory fields*, vol. II of *Course of Theoretical Physics* (Butterworth & Heinemann, New York, 1998), 4th ed.
27. Y. Chen, M. Yamaguchi, M. Wang, and X.-C. Zhang, “Terahertz pulse generation from noble gases,” *Applied Physics Letters* **91**, 251116 (2007).
28. V. S. Popov, “Tunnel and multiphoton ionization of atoms and ions in a strong laser field (keldysh theory),” *Physics-Uspekhi* **47**, 855 (2004).
29. V. S. Popov, “Multiphoton ionization of atoms by an ultrashort laser pulse,” *JETP Letters* **73**, 1–5 (2001).
30. This condition can be re-written as $c E_{\omega}^2/8\pi \gg (\alpha^8 m c^3/32\pi r_e^3)(J/J_H)^3/(J/\hbar\omega)^2$, where α is the fine structure constant, r_e classical electron radius, J/J_H the ratio of the potential of ionization to that of the atom of hydrogen, $J/\hbar\omega$ the number of photons required for the ionization. Numerically, this condition means that the laser power flux density should exceed $8.8 \times 10^{15}(J/J_H)^3/(J/\hbar\omega)^2$ W/cm².
31. N. Karpowicz and X.-C. Zhang, “Coherent terahertz echo of tunnel ionization in gases,” *Phys. Rev. Lett.* **102**, 093001 (2009).

32. C.Cuthbertson and M.Cuthbertson, "On the refraction and dispersion of krypton and xenon and their relation to those of helium and argon," Proc.Roy.Soc. **A84**, 2805–2807 (1910).
33. C.Cuthbertson and M.Cuthbertson, "On the refraction and dispersion of neon," Proc.Roy.Soc. **A83**, 149–151 (1910).
34. S. A. Korff and G. Breit, "Optical dispersion," Rev. Mod. Phys. **4**, 471–503 (1932).
35. E.R.Peck and D.J.Fisher, "Dispersion of argon," JOSA **54**, 1362–1364 (1964).

Published by
OSA

Figures

Figure 1 Angular distribution of the THz radiation computed by Equation (29) for $L/\lambda = 50$: a) driving force is directed along the plasma filament, b) driving force is perpendicular to the plasma filament.

Figure 2 Dependence of the THz field amplitude generated in the Xe versus the gas pressure. On figure, open squares correspond to the 980 mW and the dark triangles to the 600 mW of the overage power of the ω fundamental field.

Published by
OSSA

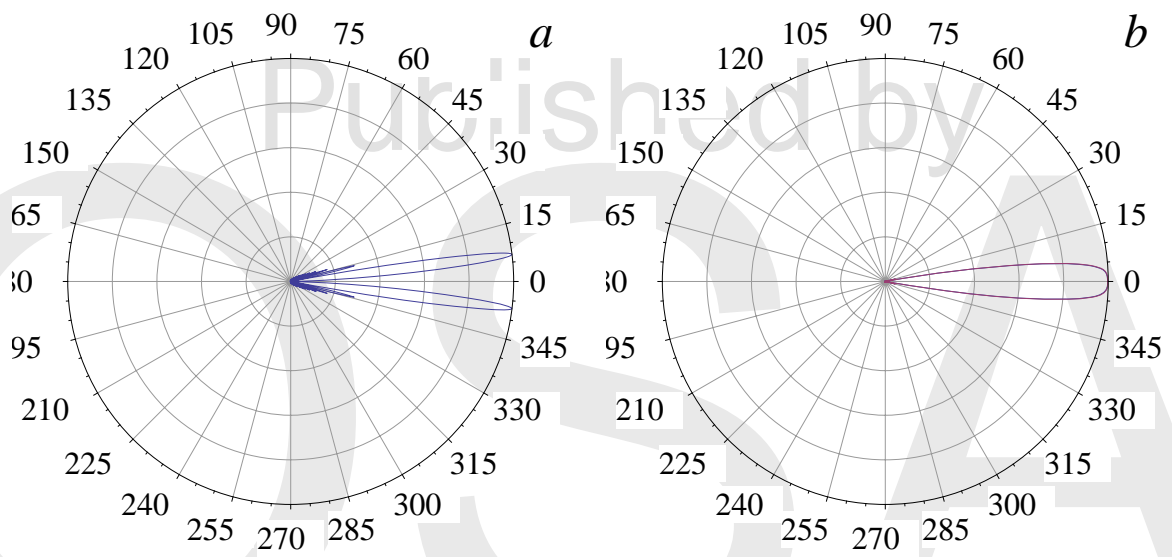


Fig. 1.

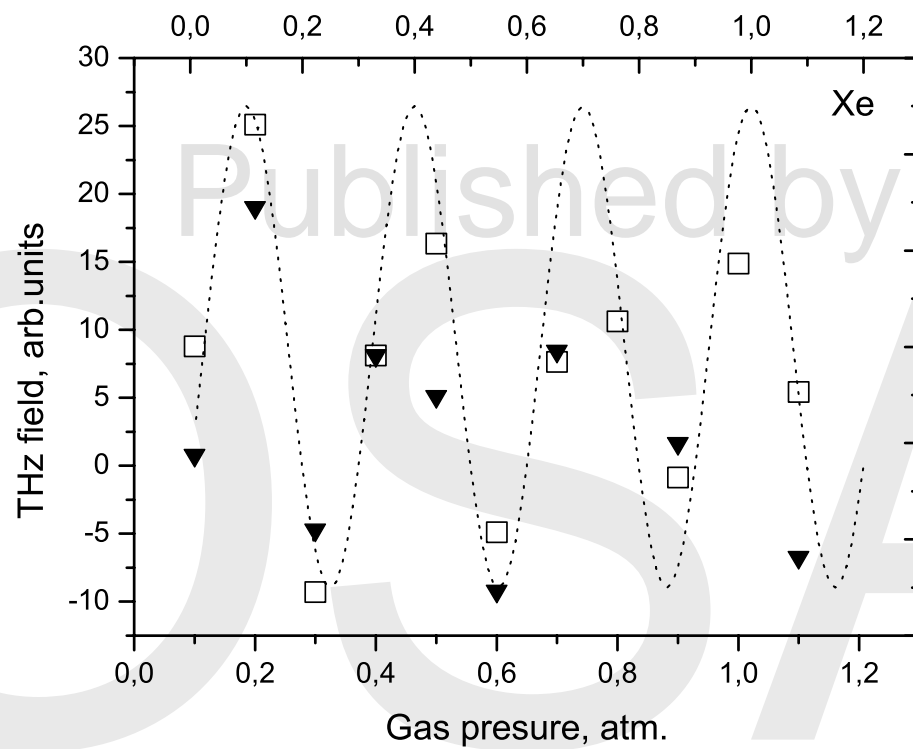


Fig. 2.